SERI/TP-211-3656
DE90000314

February 1990

Improvement of Small-Area, Amorphous-Silicon Thin-Film Photovoltaics on Polymer Substrate

Final Subcontract Report
1 March 1988 - 30 June 1989

M. F. Weber
3M Laboratories
St. Paul, Minnesota

Prepared under Subcontract No. ZB-8-07271-1

Solar Energy Research Institute
A Division of Midwest Research Institute

1617 Cole Boulevard
Golden, Colorado 80401

Operated for the
U.S. Department of Energy
under Contract No DE-AC02-83CH10093

DISCLAIMER

This report was prepared as an account of work sponsored by an agency of the United States Government. Neither the United States Government nor any agency thereof, nor any of their employees, makes any warranty, express or implied, or assumes any legal liability or responsibility for the accuracy, completeness, or usefulness of any information, apparatus, product, or process disclosed, or represents that its use would not infringe privately owned rights. Reference herein to any specific commercial product, process, or service by trade name, trademark, manufacturer, or otherwise does not necessarily constitute or imply its endorsement, recommendation, or favoring by the United States Government or any agency thereof. The views and opinions of authors expressed herein do not necessarily state or reflect those of the United States Government or any agency thereof.

DISCLAIMER

Portions of this document may be illegible in electronic image products. Images are produced from the best available original document.

SERI/TP-211-3656
UC Category: 271
DE90000314

SERI/TP--211-3656

DE90 000314

Improvement of Small-Area, Amorphous-Silicon Thin-Film Photovoltaics on Polymer Substrate

Final Subcontract Report
1 March 1988 - 30 June 1989

M. F. Weber
3M Laboratories
St. Paul, Minnesota

February 1990

SERI Technical Monitor: W. Luft

Prepared under Subcontract No. ZB-8-07271-1

Solar Energy Research Institute
A Division of Midwest Research Institute

1617 Cole Boulevard
Golden, Colorado 80401-3393

Prepared for the
U.S. Department of Energy
Contract No. DE-AC02-83CH10093
Prepared under Task No. PF931010

MASTER

DISTRIBUTION OF THIS DOCUMENT IS UNLIMITED

This publication was reproduced from the best available camera-ready copy submitted by the subcontractor and received no editorial review at SERI.

NOTICE

This report was prepared as an account of work sponsored by an agency of the United States government. Neither the United States government nor any agency thereof, nor any of their employees, makes any warranty, express or implied, or assumes any legal liability or responsibility for the accuracy, completeness, or usefulness of any information, apparatus, product, or process disclosed, or represents that its use would not infringe privately owned rights. Reference herein to any specific commercial product, process, or service by trade name, trademark, manufacturer, or otherwise does not necessarily constitute or imply its endorsement, recommendation, or favoring by the United States government or any agency thereof. The views and opinions of authors expressed herein do not necessarily state or reflect those of the United States government or any agency thereof.

Printed in the United States of America
Available from:
National Technical Information Service
U.S. Department of Commerce
5285 Port Royal Road
Springfield, VA 22161

Price: Microfiche A01
Printed Copy A03

Codes are used for pricing all publications. The code is determined by the number of pages in the publication. Information pertaining to the pricing codes can be found in the current issue of the following publications which are generally available in most libraries: *Energy Research Abstracts (ERA)*; *Government Reports Announcements* and Index (*GRA* and I); *Scientific and Technical Abstract Reports (STAR)*; and publication NTIS-PR-360 available from NTIS at the above address.

PREFACE

This report covers the work performed by the Applied Technologies Laboratory of the 3M Company to improve the performance of p-i-n solar cells deposited on polyimide substrates. The contract period was from 1 March, 1988 to 30 June, 1989. The project manager is Dr. Donald L. Janes and the principal investigator is Dr. Michael Weber.

Other individuals who have contributed to this project include:

Dr. Kenneth Epstein

Mr. James Gilbert

Dr. Frank Jeffrey

Mr. Francis McFadden

Mr. Lawrence McGraw

Mr. Richard Thompson

SUMMARY

Objectives

The overall objective of this one-year contract was to produce, using roll-to-roll deposition on polyimide substrate, a small-area, amorphous–silicon p-i-n photovoltaic cell with an energy conversion efficiency of 10 percent under AM 1.5 insolation. To achieve this goal, improvements were needed in three main areas. Briefly these were: 1) transparent conductive oxide (TCO) top contact, 2) red light response of the cell, and 3) improvements in the fill factor of reverse structured cells (p^+ layer deposited last).

Discussion

Problems with contact resistance of the SnO_2/ITO top contact were eliminated by switching to zinc oxide (ZnO) as the transparent conducting top contact. In addition, the ZnO conductivity was improved to produce a TCO of 8 to 9 ohms/square sheet resistance with less than 8 percent average optical absorption. Following these improvements, p-i-n cells with fill factors above 0.70 were routinely fabricated.

Progress was also made in improving the red light response of the cells. Dielectric enhanced metal reflecting electrodes increased the short circuit current density by over 1mA/cm^2. In addition, a three-layer dielectric mirror coating was designed which can increase the current density by an additional 1mA/cm^2, although this has not yet been demonstrated on a device. The highest current density measured at SERI on our cells was 14.3 mA/cm^2. The highest efficiency demonstrated on a device was 8.36%.

Some progress was made in the third area: improving the fill factor of the n-i-p (reverse structured) devices made in the multi-chamber deposition system. Although high fill factors were achieved with p-i-n devices made in a single-chamber system, stability and manufacturing requirements demand an n-i-p cell fabricated on a continuously moving substrate in a multi-chamber system. The latter devices are currently limited by fill factors of 0.67 and open circuit voltages of 0.89 volt.

Conclusions

The overall goal of 10% efficiency on a small-area cell was not achieved. The highest efficiency demonstrated was 8.36%. The major obstacles to achieving 10% efficiencies with our cell structure and fabrication processes are: 1) controlling thin film defects which cause electrical shunts in devices fabricated on enhanced reflection electrodes, and 2) controlling impurities and introducing dopant profiles near the p/i interface in a continuous web deposition system.

TABLE OF CONTENTS

Section		Page
1.0	INTRODUCTION	1
2.0	EXPERIMENTAL	3
3.0	RESULTS AND DISCUSSION OF WORK PERFORMED	9
3.1	Transparent Conducting Electrodes	9
3.1.1	Contact Resistance	9
3.1.2	ZnO: Preparation and Properties	11
3.1.3	ZnO: Stability	15
3.2	Device Performance	15
3.3	Enhanced Reflectivity Metal Electrodes	17
3.4	Reverse Structure Cells and the Multi-Chamber Deposition System	25
3.4.1	Deposition Rate	26
3.4.2	p/i Interface	28
4.0	CONCLUSIONS	29
5.0	REFERENCES	30

LIST OF FIGURES

Figure		Page
1.	Standard substrate coatings with p-i-n a-Si cell deposited thereon.	4
2.	General Construction of n-i-p Solar Cells on Polyimide Substrate	5
3.	Single-chamber Silicon Deposition System.	6
4.	Schematic of Multi-chamber Silicon Deposition System	7
5.	Schematic Outline of CVD Roll-to-roll Web Coater for Depositing Conducting ZnO Films	8
6.	SEM Micrograph of the CVD ZnO surface.	12
7.	Reflection and Transmission of ZnO on Polyester.	13
8.	Reflection Spectra of Cells with the Standard Construction shown in Figure 1.	14
9.	I-V Curve of a Cell with the Construction : Polyimide/Al/TiN/p-i-n Si/ ZnO, with an i-layer 5000 angstroms thick.	16
10.	I-V Curve for the highest efficiency cell produced with our construction on polyimide substrate.	17
11.	Computer Modeled Optical Absorption Spectra of the bottom electrode in a n-i-p solar cell with quarterwave ITO top contact.	18
12.	Optical Absorption in a silver electrode.	19
13.	Computer Modeled Optical Absorption Spectra of the bottom electrode of a n-i-p solar cell, assuming the incident medium has an index of n=4.0	19
14.	Optical Absorption Spectra, comparing bare aluminum with single layer dielectric and triple layer dielectric enhanced films.	20
15.	Spectral Response Curves for n-i-p a-Si solar cells on specular and various textured surfaces. The response is normalized to 1.0 at the peak efficiency point.	22
16.	SEM Micrograph of the optimum textured aluminum substrate for enhancing the red light response of the n-i-p solar cells.	23

LIST OF FIGURES (continued)

Figure **Page**

17. Total and Diffuse Reflectance Spectra for the silver coated textured aluminum surface in Figure 16. 24

18. Schematic End View of i-chamber with double magnet array. 27

LIST OF TABLES

Table **Page**

1. Comparison of Various Top Contacts 10

2. Comparison of Short Circuit Current Densities (mA/cm^2) for devices on various textured metal electrodes. 21

1.0 INTRODUCTION

At the start of 3M's amorphous-silicon solar cell program in 1983, sputtered indium tin oxide (ITO) was chosen for the transparent conductor to form the top contact to the solar cell. The high deposition rate, high electrical conductivity, optical transparency, and low deposition temperature of sputtered ITO led to this choice. Very early in the program, however, it became apparent that indium could diffuse into the silicon and substantially lower the fill factor. Sputtered tin oxide (SnO_2) was selected as a good indium diffusion barrier, but good ohmic contact to the silicon was never reproducibly achieved with this material. The SnO_2 was sputtered from a tin metal target with an argon/oxygen plasma. It became obvious that sputter depositing SnO_2 on silicon in an oxidizing atmosphere of oxygen and argon was a very different problem than most other groups faced, i.e. depositing silicon onto SnO_2 in a reducing atmosphere of hydrogen. A material, and method of deposition, was then sought to replace the sputtered SnO_2 as the contact layer to the silicon.

Solving the contact problem between the TCO and silicon was the first objective of this contract. Quantitatively, the goal was to produce cells with fill factors equal to or greater than the fill factors obtained on cells with semi-transparent chromium contacts. Chromium is known to have a low contact resistance to silicon and is very easy to evaporate onto small samples in a semi-transparent state at a thickness of 100 angstroms. A zinc oxide (ZnO) contact made by the Chemical Vapor Deposition technique (CVD) was found to meet this goal.

The second objective of this contract was to increase the short circuit current density of the devices by improving their efficiency in the 600 nm to 800 nm region of the spectrum.

Two main properties of a metal substrate determine the red light response of p-i-n solar cells fabricated on that substrate. These two variables are substrate texture (microgeometry of the surface) and reflectivity of the metal. Both features are critical in obtaining high short circuit current densities, but the latter is especially important for cells constructed on opaque substrates as opposed to cells fabricated on transparent "superstrates". (See Figures 1 and 2 for illustrations of our cell structures on polyimide.) For optimized cells of each type, the short circuit density of a cell with the structure polyimide/textured Al/n-i-p/TCO is less than the short circuit current density of a cell with the structure glass/textured TCO/p-i-n/Al, even though both have aluminum as reflecting electrodes. The difference is in the texture on the aluminum, and therefore in the parasitic optical absorption of the aluminum. The only obvious

solution for improving cells with opaque substrates is to increase the reflectivity of the textured aluminum to decrease its optical absorption. This is the approach we have pursued.

2.0 EXPERIMENTAL

The 3M amorphous silicon cell is based on a 2-mil thick, 4-inch wide polyimide film. With roll-to-roll technology, a flexible film of material, whether paper, plastic or metal, is usually referred to as the "web". The outgassing of the polyimide web is a prerequisite to achieve high-efficiency solar cells. For the 3M cell, a thermal outgassing of the polyimide, followed by a proprietary web treatment, provides a relatively inert substrate. The web treatment and metallization is done in one roll-to-roll machine. The metal layers are sputtered on as the web moves past a series of standard d.c. magnetron sputtering cathodes.

For much of our development work, a "standard" substrate was employed, consisting of specular and textural aluminum layers overcoated with a thin layer of titanium nitride.

The textured aluminum can be deposited from high purity aluminum targets with substrate temperatures from 150°C to 200°C. More details are given below in Section 3.3. To provide good continuity of the metal and to provide more spherical features to the texture, an aluminum alloy was sputtered on the web both before and after the textured aluminum layer. Sputtered aluminum alloys produce very smooth thin films.

The standard substrate, coated with a p-i-n cell and TCO, is illustrated in Figure 1. The thin titanium nitride layer serves as a diffusion barrier to prevent the aluminum from mixing with the silicon. Aluminum diffuses rapidly in silicon at the 230°C deposition temperature of the amorphous silicon.

TCO	
n^+ microcrystalline Si	0.02
intrinsic silicon	0.50
p^+ microcrystalline Si	0.03
Titanium Nitride	0.01
Aluminum Alloy	0.05
Textured Aluminum	0.30
Aluminum Alloy	0.05
Polyimide	50.0

Figure 1. <u>Standard substrate coatings with p-i-n a-Si cell deposited thereon.</u> TCO thickness depends on the material chosen for that layer. See Table 1 and text for typical values.

In this text, the sequence of letters p-i-n and n-i-p will be used to denote the sequence of silicon film deposition. Thus p-i-n refers to a cell with the n^+ silicon layer deposited last. With an opaque substrate, light must enter this cell through the n^+ layer. p-i-n cells on glass substrates are configured so light passes first through the p^+ layer. This latter configuration is known to lessen the impact of the Staebler-Wronski effect. To achieve this advantage with opaque substrates, a so-called "reverse-structure" cell, or n-i-p configuration, is utilized. This construction is illustrated in Figure 2. Also illustrated in Figure 2 are extra metal and oxide layers for enhancing the reflectivity of the substrate. The top aluminum alloy layer of Figure 1 is shown replaced by layers of titanium, silver, and zinc oxide. The titanium layer is simply for improved adhesion of silver, and the zinc oxide is a quarterwave thick film to enhance the reflectivity of the

silver. This effect is discussed in detail in Section 3.3. The cell in Figure 2 is shown with a thick ZnO film which provides a 10 ohm/square TCO.

Zinc Oxide	1.60
p^+ microcrystalline Si	0.03
intrinsic Silicon	0.50
n^+ microcrystalline Si	0.02
Zinc Oxide	0.06
Silver	0.10
Titanium	0.05
Textured Aluminum	0.30
Aluminum Alloy	0.05
Polyimide	50.0

Figure 2. <u>General construction of n-i-p Solar Cells on Polyimide Substrate.</u> Thickness values are given in micrometers. The standard construction does not include the silver and zinc oxide bottom electrode films, in which case TiN is deposited instead of titanium.

For this contract, all p-i-n cells were deposited in a small single-chamber vacuum system, illustrated in Figure 3. All three silicon layers were deposited sequentially on a stationary web. Operating much like film in a camera, up to 30 "frames" (complete 4" x 4" cells) could be deposited on a continuous web before breaking vacuum.

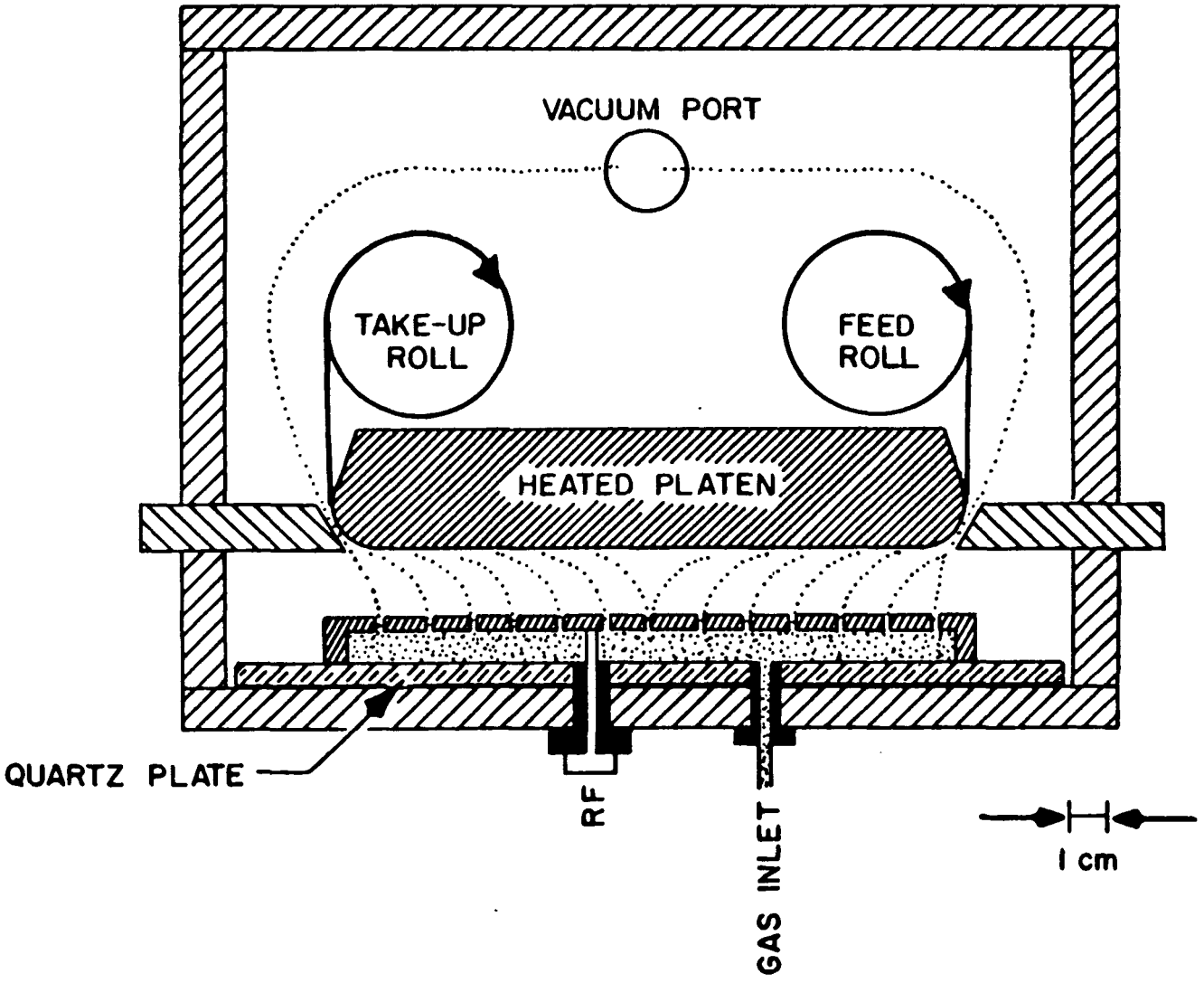

Figure 3. Single-chamber silicon deposition system. p-i-n cells are deposited frame-by-frame in a step-and-repeat fashion.

The design of the single-chamber system does not permit fabrication of high quality n-i-p devices. The highest fill factor on such a device from this system was 0.50. So, unless otherwise noted, all n-i-p cells fabricated under this contract were deposited in one pass through the silicon multi-chamber deposition system, shown in Figure 4. The various layers are deposited in the individual mini-chambers as the web passes through. Experiments to improve the fill factor of the devices have required the

addition of two more "mini-chambers". There are now five separate chambers for deposition of n^+, p^+, i, and two buffer/transition layers in one continuous pass of the web through the system. The intrinsic silicon layer is now enclosed and protected from the outer vacuum-can environment (PH_3, B_2H_6 and background gasses) as it passes from the intrinsic silicon deposition zone to the p^+ deposition zone. The 5 mini-chambers, and the length of the plasma zone in each, in sequence as the web travels, are: n^+ (4-inch zone), i (14-inch zone), buffer (7-inch zone), i/p^+ transition shroud (4-inch zone), and p^+ (7-inch zone). The i and buffer chambers are built in one unit, i.e. no gap exists between the i and buffer chambers, as shown in Figure 4. The i/p^+ transition shroud was placed where the idler roller is shown between the i and p^+ chambers. The shroud area has its own r.f. electrode and gas supply manifold.

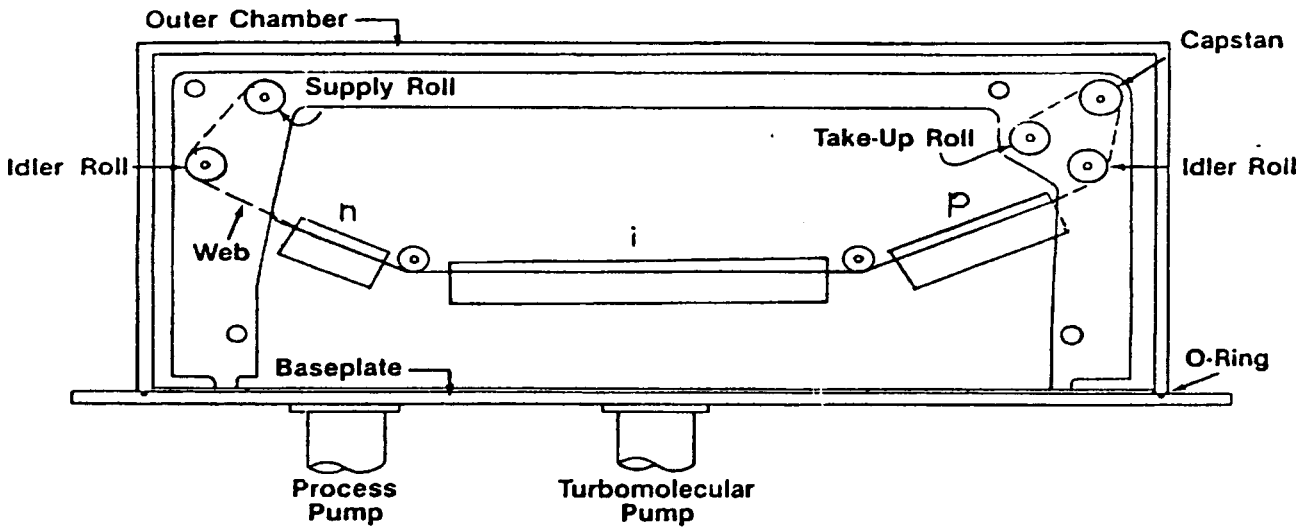

Figure 4. <u>Schematic of multi-chamber silicon deposition system.</u> The i-chamber, shown as one unit, actually has two compartments separated by an internal slit which the web passes through. The i/p^+ transition shroud was placed where the idler roller between the i and p chambers is shown.

The "mini-chamber" or slit isolated chamber-within-a-chamber concept was utilized to construct the ZnO deposition system as well. Whereas the silicon is deposited by plasma assisted CVD, the ZnO is deposited strictly by thermal CVD, but with roughly the same pressures and flow rates as the silicon systems. A schematic of the ZnO deposition chamber and web-drive system is shown in Figure 5. The web is drawn

under a heated curved platen where it is exposed to the vapors necessary for depositing ZnO. The system has a 14-inch long deposition zone.

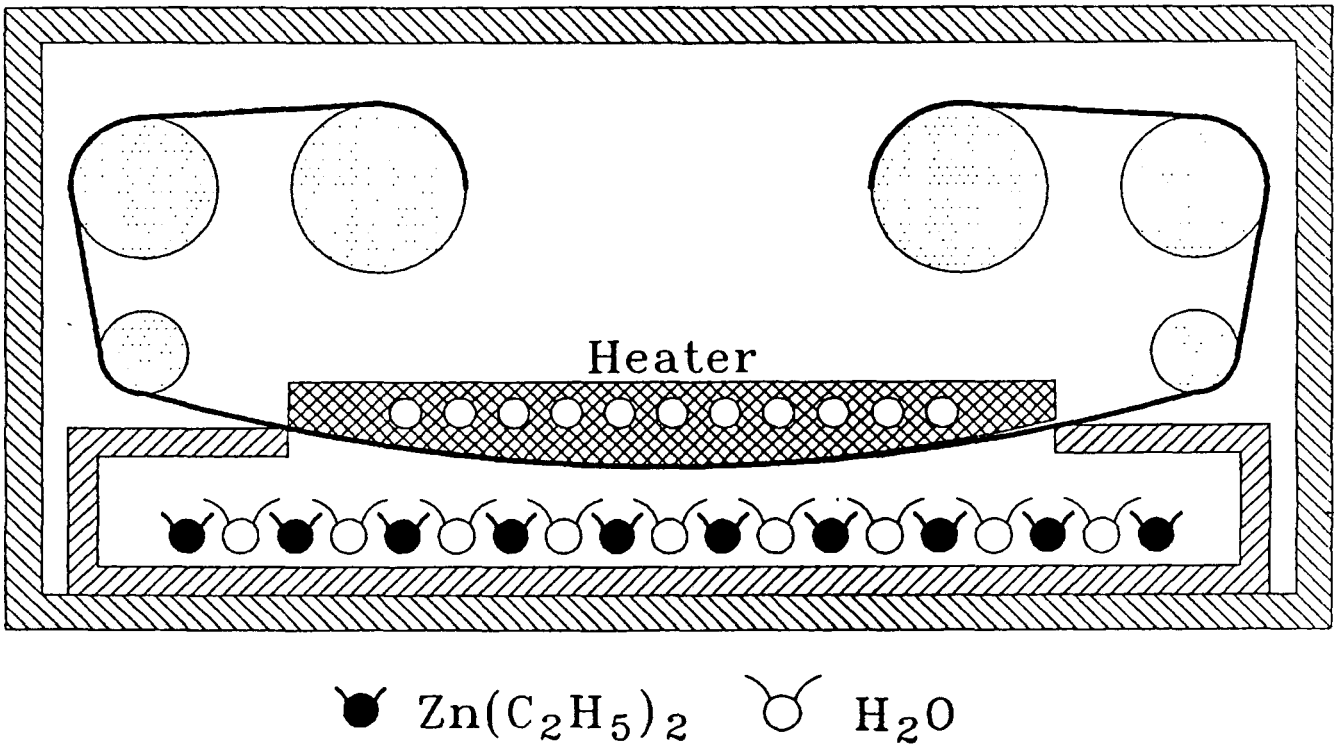

Figure 5. <u>Schematic outline of CVD roll-to-roll web coater for depositing conducting ZnO films.</u>

Thin film growth of ZnO by organometallic chemical vapor deposition (with diethylzinc and H_2O) was first reported in 1980 by C.K. Lau, S.K. Tiku and K.M. Lakin [1]. It has long been known that a group 3A element (indium) can be used to provide a stable doping of ZnO [2, 3, 4]. Boron was used to dope the films described here, as diborane was readily available in the lab. Argon is used as a carrier gas for both the water vapor and the diethylzinc.

3.0 RESULTS AND DISCUSSION OF WORK PERFORMED

3.1 Transparent Conducting Electrodes

With the cell construction shown in Figure 1, light is most effectively coupled into the silicon with a quarterwave thick transparent conductor. Quarterwave here refers to the center of the visible spectrum, approximately 550 nm wavelength. The lowest sheet resistance obtainable with such a film, with minimal optical absorption, is about 100 ohms/square with indium tin oxide (ITO). However, on a module, such a construction requires metallic current collecting grids which cover about 5 to 10% of the surface. With careful control of the deposition conditions, ITO can be deposited in thicker films which have only 10 ohms/square sheet resistance and less than 10% absorption, but the high deposition rates required usually cause sample heating which induces indium diffusion into the silicon, causing an electrical barrier. To stop the diffusion of indium, a tin oxide barrier layer must first be sputtered on. This latter process produced an objectionably high contact resistance to the silicon. This added resistance causes a reduction of the device's fill factor. In addition to a high contact resistance, our research prior to this contract indicated that the sputtering process itself also lowered the cell's fill factor via some sort of plasma-induced damage to the p/i interface that could not be thermally annealed out.

The use of specially designed magnetron sputtering targets reduced the plasma induced damage, but did not eliminate it. This problem was circumvented with the use of chemical vapor deposited (CVD) boron-doped ZnO as the contact layer to the doped silicon p^+ (or n^+) layer.

At the start of the contract, cells with ZnO/Cr and ZnO/ITO two-layer transparent electrodes were tested. Later, when the conductivity of the ZnO was increased to provide 10 ohms/square sheet resistance, only ZnO was used in the top electrode.

3.1.1 CONTACT RESISTANCE

Table 1 lists the fill factors for 4 different sets of a-Si devices contacted with various materials used as transparent electrodes. The comparison within each set is between otherwise identical samples. The first set compares chrome to ZnO/chrome contacts. The second set compares SnO_2 and ZnO used as both a contact and diffusion barrier between silicon and ITO. Sets one and two are for cells with the p^+ layer contacting the transparent electrode. The third set compares results for small area (0.04 cm^2) chrome contacted cells to 0.37 cm^2 ZnO contacted cells having the

n^+ layer in contact with the transparent electrode. The ZnO had a sheet resistance of 10 ohms/square. Set number four includes only one type of sample -- one with 10 ohms/square ZnO as both a top and bottom electrode. In all cases, we see that the ZnO produces a higher fill factor due to its low contact resistance to either p^+ or n^+ doped silicon layers. The n^+ and p^+ layers are microcrystalline silicon except for the last case, which required an amorphous silicon p^+ layer to be deposited on the ZnO. The high power densities required to produce a microcrystalline layer were found to cause an electrical barrier at the ZnO/Si interface when depositing microcrystalline silicon onto ZnO. This barrier problem was solved later in the contract period by the prior deposition of a thin, doped amorphous silicon layer onto the ZnO.

TABLE 1. Comparison of Various Top Contacts.

Device Type	Bottom Contact	Top Contact	Fill Factor	Top Contact Thickness
n-i-p	TiN	Cr	0.65	100 Å
n-i-p	TiN	ZnO/Cr	0.67	150 Å/100 Å
n-i-p	TiN	SnO_2/ITO	0.57	100 Å/2200 Å
n-i-p	TiN	ZnO/ITO	0.66	150 Å/2200 Å
p-i-n	TiN	Cr	0.69	100 Å
p-i-n	TiN	ZnO	0.70	1.6 micrometers
p-i-n	ZnO	ZnO	0.70	1.6 micrometers

A very interesting effect was found to occur with ZnO contacted n-i-p cells (p^+ microcrystalline layer on top). Typical $V_{o.c.}$'s for these cells are 0.88 volt with a standard p^+ layer. If the p^+ layer was made thinner, so that $V_{o.c.}$ drops to as low as 0.75 volt when contacted with chromium, contact with the n-type ZnO on identical samples raised the voltage to as high as 0.84 volt. A possible explanation of this restoration of $V_{o.c.}$ may lie with the common dopant (boron) for p^+ silicon and the n^+ ZnO. The deposition temperature of the ZnO (177°C) is higher than that for the p^+ silicon (160°C) and may result in some boron diffusion into the silicon. Further research is required to verify this hypothesis.

3.1.2 ZnO: PREPARATION AND PROPERTIES

The low contact resistance of ZnO to p-i-n a-Si devices has made it the preferred top contact for our polymer-based photovoltaic cells. Until recently, the ZnO was not conductive enough to function alone as the sole component of the TCO. During this contract period the conductivity and stability were improved enough so that 10 ohms/square could be obtained with a 10-minute deposition (~ 1.6 micrometers).

The conductivity was improved by a systematic variation of substrate temperature, partial pressures of H_2O and $Zn(C_2H_5)_2$, total gas flow rates, and gas mixing conditions. The deposition rate and optical absorption increased monotonically with increasing substrate temperature. For the conditions we explored, the sheet resistance for a 1.6 micrometer thick film reached a minimum for substrate temperatures between 175°C and 180°C. At 177°C the deposition rate was ~25 Å/second and a 1.6 micrometer film had 8 to 9 ohms/square sheet resistance. With a continuously moving web, the downweb uniformity was $\pm$ 5% while the crossweb uniformity was slightly better than $\pm$ 10%. For a substrate temperature of 150°C, a 1.6 micrometer thick film gave approximately 30 ohms/square sheet resistance.

The relationship between sheet resistance and film thickness for the ZnO is nonlinear, with resistance going up steeply for very thin films. As stated above, a 1.6 micrometer film gave $\leq$ 10 ohms/square, but 0.16 micrometer films measured 500 ohms/square, and quarterwave thick films (0.07 micrometer) measured 2000 ohms/square. Furthermore, when baked for 20 hours at 100°C in air, R (for 0.16 micrometer films) increased to 1500 ohms/square whereas the 10 ohms/square material did not change noticeably. So for the present, use of quarterwave thick ZnO as a TCO is not possible and the 1.6-micrometer thick, 10 ohms/square is the standard TCO.

The poor stability and high resistance of the very thin films may possibly be linked to the structure of these films. A large grain size and rough surface texture is characteristic of ZnO films produced by reacting water vapor with diethyl zinc. An SEM micrograph is displayed in Figure 6, which shows grain sizes between 0.25 and 0.35 micrometer. The nonlinearity and instability of the sheet resistance was observed on films thinner than these grain sizes.

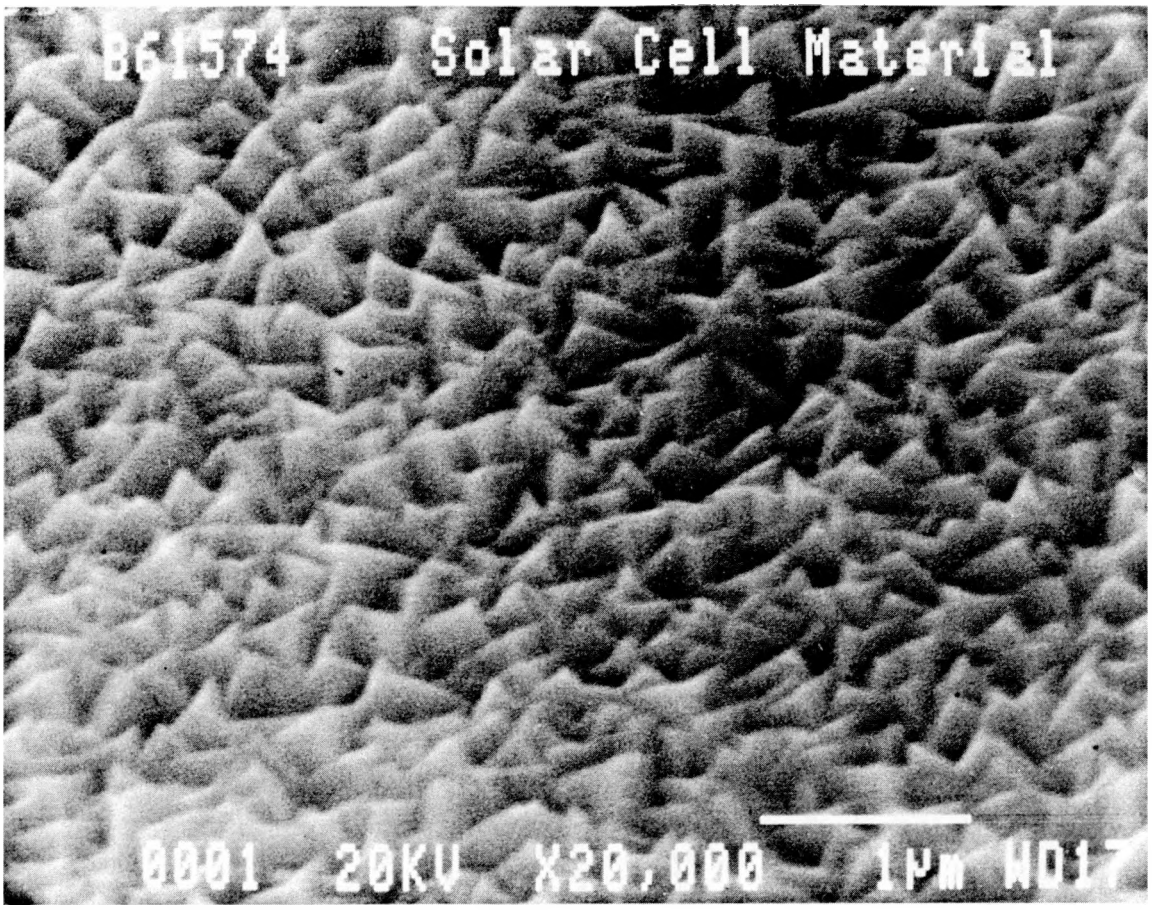

Figure 6. <u>SEM Micrograph of the CVD ZnO Surface.</u> The ZnO is 1.6 micrometers thick and the grain sizes are between 0.25 and 0.35 micrometer.

The optical absorption increased slowly as the deposition temperature of the ZnO was increased. For films deposited at 150°C, the average absorption from 400 to 800 nm was approximately 6%. The optical reflection and transmission curves of a ZnO film deposited at 150°C (1.6 micrometer thick) are shown in Figure 7. The substrate was a 3M fluorinated polyester (FPE) film. Sheet resistance was ~ 30 ohms/square. At higher substrate temperatures, a pre-outgassed polyimide film was utilized as the substrate. The average optical absorption of films deposited at 177°C was 8%. The average was taken from measurements between 500 and 800 nm as the polyimide was opaque below 500 nm. The absorption was constant across the observed spectrum however, similar to that in Figure 7. Although the optical absorption in ZnO films grown at 177°C was slightly higher than for films grown at 150°C (8% versus 6%), the lower sheet resistance of 10 ohms/square versus 30 ohms/square determined the selection of the higher growth temperature for the ZnO.

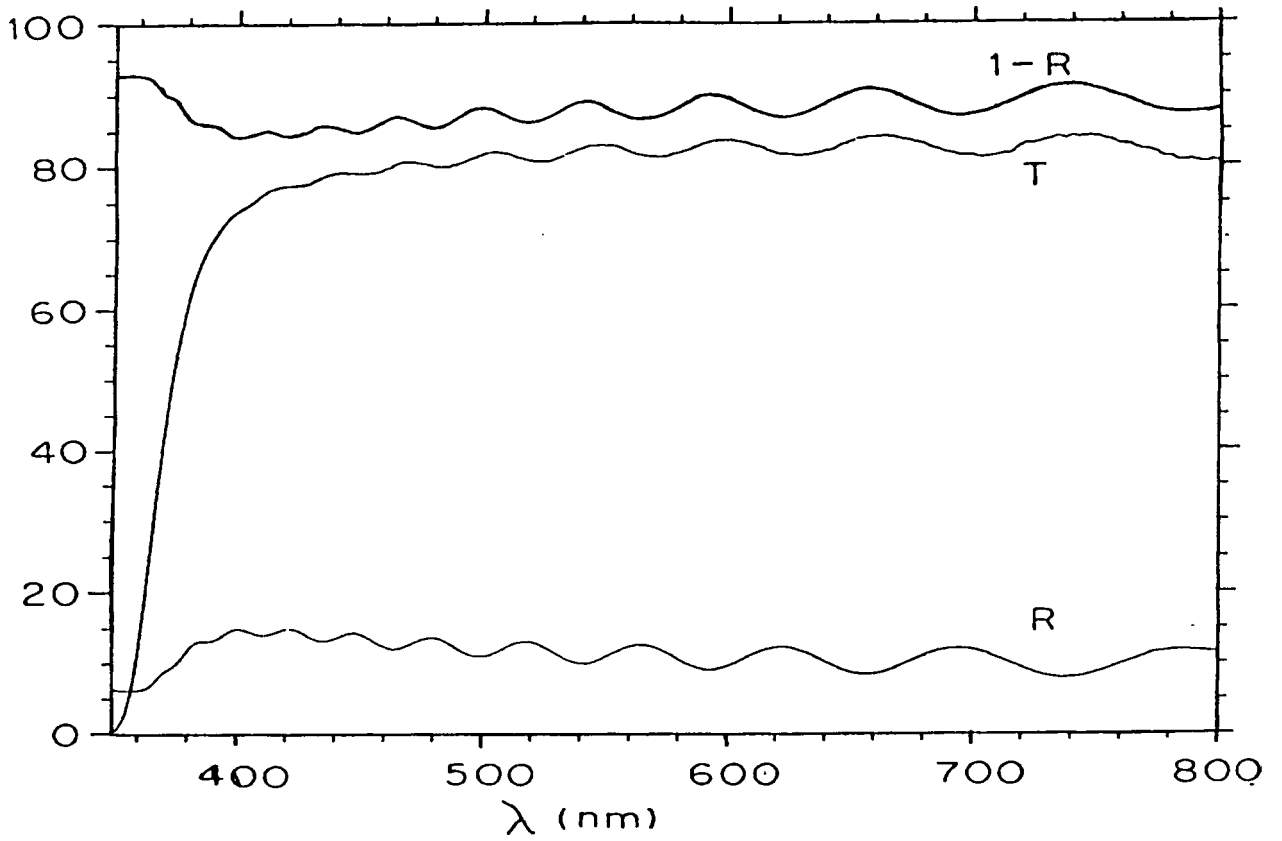

Figure 7. <u>Reflection and Transmission of ZnO on Polyester.</u> The absorption is the difference between the 1-R and the T curves. These data are for ZnO deposited at 150°C. The average optical absorption between 400 nm and 800 nm is 6%.

Besides the optical absorption in the ZnO, there is also approximately a 5% reflection from the silicon/ZnO interface. This number was inferred from an analysis of the two reflection curves shown in Figure 8. The upper curve is the reflection from a cell with the construction of Figure 1, using ZnO (1.6 micrometer thick) as the TCO. The ZnO layer, not being a quarterwave thick, is not the most effective anti-reflection coating for silicon. The texture at the top surface of the silicon (resulting from the aluminum texture) and the texture at the top surface of the ZnO, both work as graded index anti-reflection coatings, resulting in the average measured reflectance of about 8%. If the ZnO is coated with a quarterwave thick film of MgF_2 (n=1.39), the reflection off the top of the ZnO should be reduced practically to zero, as the index of MgF_2 is very close to the square root of the index of ZnO (n=2.0). The remaining 5% reflection, given by the lower curve from 400 to 600 nm, can only come from the index mismatch at the

ZnO/Si interface. This conclusion is supported by computer modeling (on smooth films). Computer simulation also predicts that this reflection can be greatly reduced by the insertion of a layer of index n=3.0, such as silicon carbide, between the silicon and ZnO. To be effective, such a layer would have to be close to a quarterwave thick (450Å). However, the absorption losses in the blue, from 400 to 500 nm, might then exceed the gains obtained from lower reflection losses across the whole spectrum.

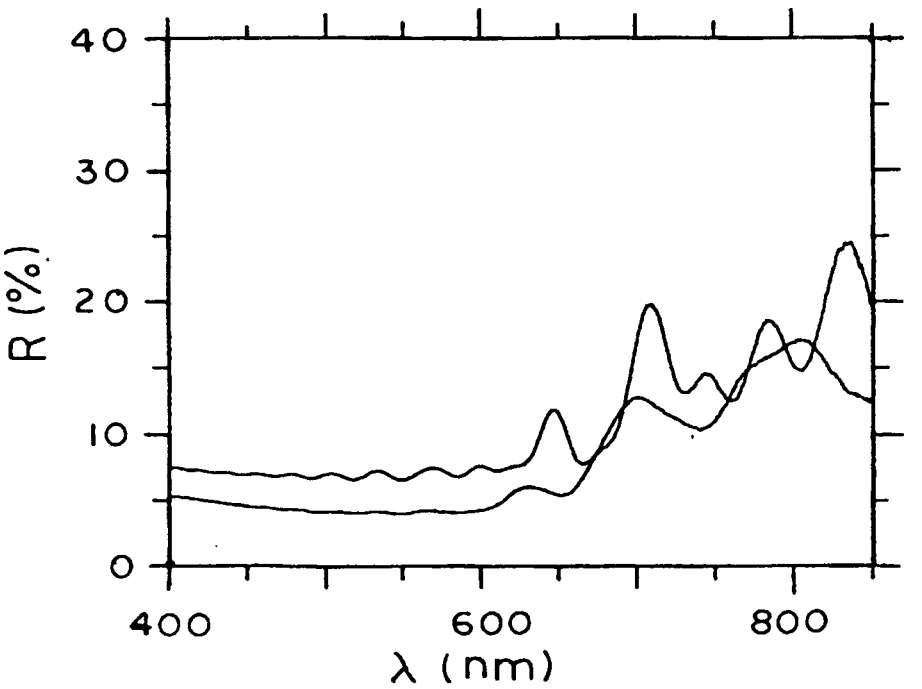

Figure 8. **Reflection spectra of cells with the standard construction, shown in Figure 1, before (top curve) and after overcoating with MgF_2 (bottom curve).**

As discussed above, the magnitude of $I_{s.c.}$ depends on which TCO is chosen to complete the cell. Quarterwave optically-thick coatings of ITO (~70 nm) produce the highest current density because of the excellent anti-reflecting properties and low absorption of this thin coating. The combined reflection and absorption losses from quarterwave thick ITO on silicon are only ~ 5%. However, the reflection is close to zero at 550 nm where the quantum efficiency of p-i-n devices is usually a maximum.

With a 10 ohms/square ZnO film for the TCO, total reflection and absorption losses are ~13% from 400 to 700 nm as discussed above. Therefore, a quarterwave coating of ITO (~700 nm) will produce the highest current densities for our cells, but as

discussed in Section 3.1.1 (see Table 1), the deposition technique results in a lower fill factor. Unless that problem can be overcome, a thick ZnO top contact will produce the highest efficiency p-i-n device with our cell configuration.

3.1.3 ZnO: STABILITY

Standard 10 ohms/square films of ZnO on silicon coated polyimide were stored in an air oven at 100°C for 7 months. After that period, the resistance was found to have increased to 12 ohms/square. Samples stored at room temperature showed no measurable degradation during the same time period. Similarly, samples stored under water at room temperature for one month showed no change in sheet resistance. The degradation at 100°C is acceptable for most outdoor applications where peak temperatures rarely exceed 75°C, although the change is cause for some concern. Further experiments should be performed to understand the degradation mechanism, and, we hope, help to eliminate it.

3.2 Device Performance

The low series resistance, coupled with the low contact resistance of ZnO films on p-i-n devices, has produced a significant increase in the fill factor of our devices. With a 10 ohms/square ZnO top contact, p-i-n devices with fill factors above 0.70 can be routinely fabricated. An I-V curve obtained at SERI is shown in Figure 9. The device structure was the same structure as illustrated in Figure 1. The current density is low (12.1 mA/cm^2) because of optical absorption in the bottom aluminum electrode and the resulting efficiency is only 7.75%. See Section 3.3 for a detailed analysis of metal electrode reflectivity. Although higher current densities are needed to produce a 10% efficient device, the ff listed in Figure 9 is significant for two reasons. First, it shows that the ZnO film growth at 177°C is compatible with our device structure, producing low TCO/Si contact resistance, high shunt resistance, and no damage to other interfaces such as the p/i interface. Secondly, it demonstrates that the polyimide substrate, when properly treated, will not interfere with the fabrication of the high quality intrinsic silicon needed for high efficiency devices. Measurements in our laboratory gave fill factors between 0.70 and 0.72 on similar devices from approximately 100 depositions in the single-chamber system (shown in Figure 3).

Sample #1753-1a

Area = 0.28 cm²

$I_{s.c.}$ = 3.389 mA

$V_{o.c.}$ = 0.8966 volt

Imax = 2.942 mA

Vmax = 0.7371 volt

Fill Factor = 71.37%

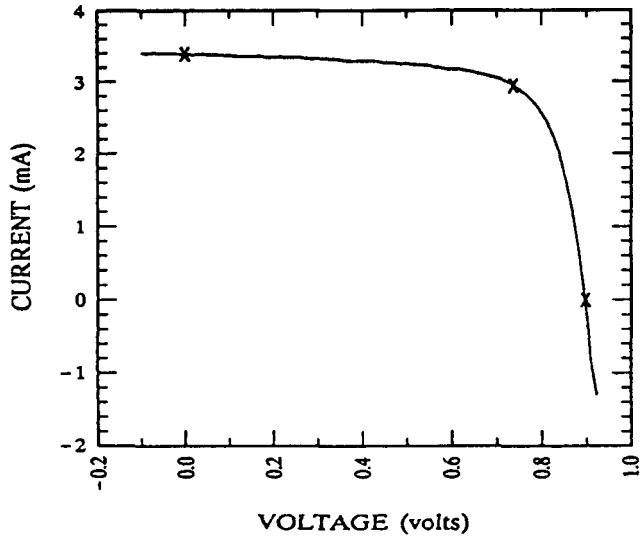

Figure 9. <u>I-V curve of a cell with the construction: polyimide/Al/TiN/p-i-n Si/ZnO, with an i-layer 5000 angstroms thick.</u> The active area was 0.28 cm² and the efficiency was 7.75%

Slightly higher efficiency is possible if the standard textured aluminum base electrode is coated with silver to increase its reflectivity. With a silver base, the best fill factor was slightly lower, 0.69, but the higher current density (13.46 mA/cm², measured at SERI) results in an efficiency of 8.36%. The I-V curve and other cell parameters are given in Figure 10.

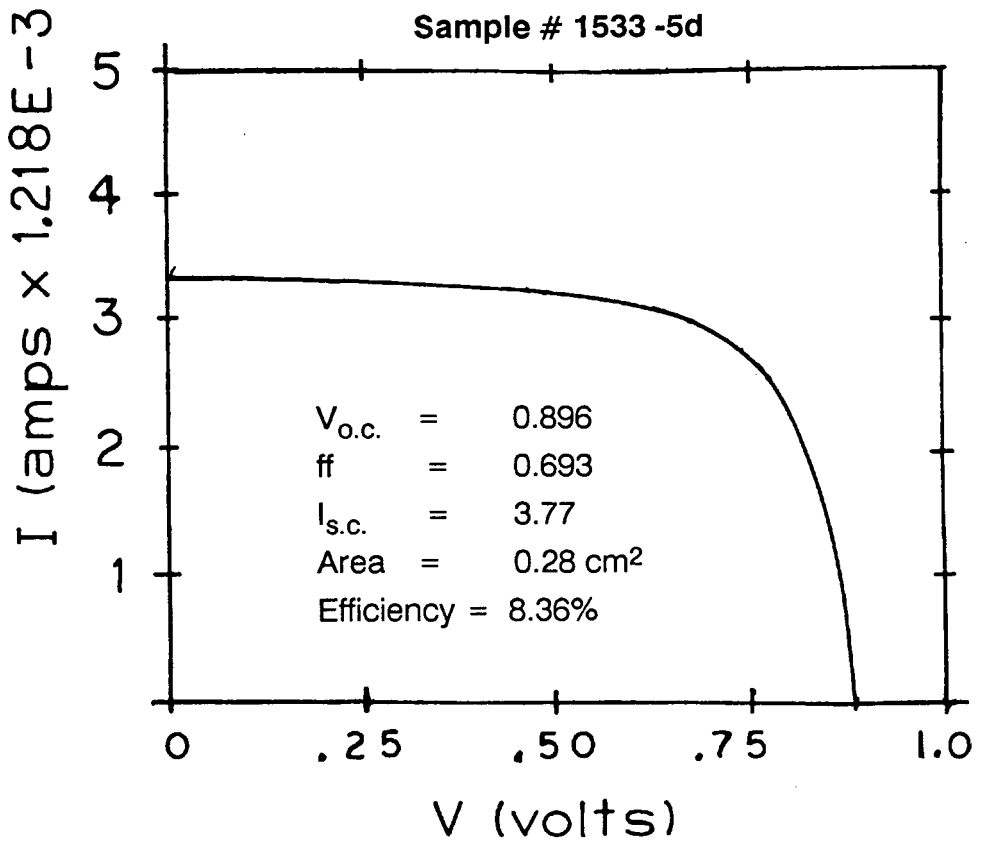

Figure 10. <u>I-V curve for the highest efficiency cell produced with our construction on polyimide substrate.</u> The current density, measured at SERI, was 13.46 mA/cm^2, giving an efficiency of 8.36%.

3.3 Enhanced Reflectivity Metal Electrodes

Substantial improvements in the red light response of the devices were obtained with dielectric enhanced metal bottom electrodes. Quarterwave thick coatings of ZnO were sputtered onto silver and aluminum coated polyimide to enhance the reflectivity of these metals. The ZnO was sputtered from a zinc metal target doped with indium. Computer modeling of the optical behavior of ZnO coated metals shows that substantial gains in reflectivity are possible, even for silver films. A three-layer dielectric film was designed and computer modeled also, and some experimental work started on it. The three-layer reflection enhancement coating consists of ZnO/a-Si/ZnO, with each layer a quarterwave thick. The a-Si was sputtered by d.c. magnetron from a 0.1 ohm-cm phosphine doped target in an Argon/Hydrogen

atmosphere. Optical modeling results for the single layer dielectric (ZnO) on metal are shown in Figures 11, 12, and 13. All absorption curves are the total optical absorption in all layers below the n-i-p device, as a percentage of light incident on the device from above. The devices are variations of the structure illustrated in Figure 2.

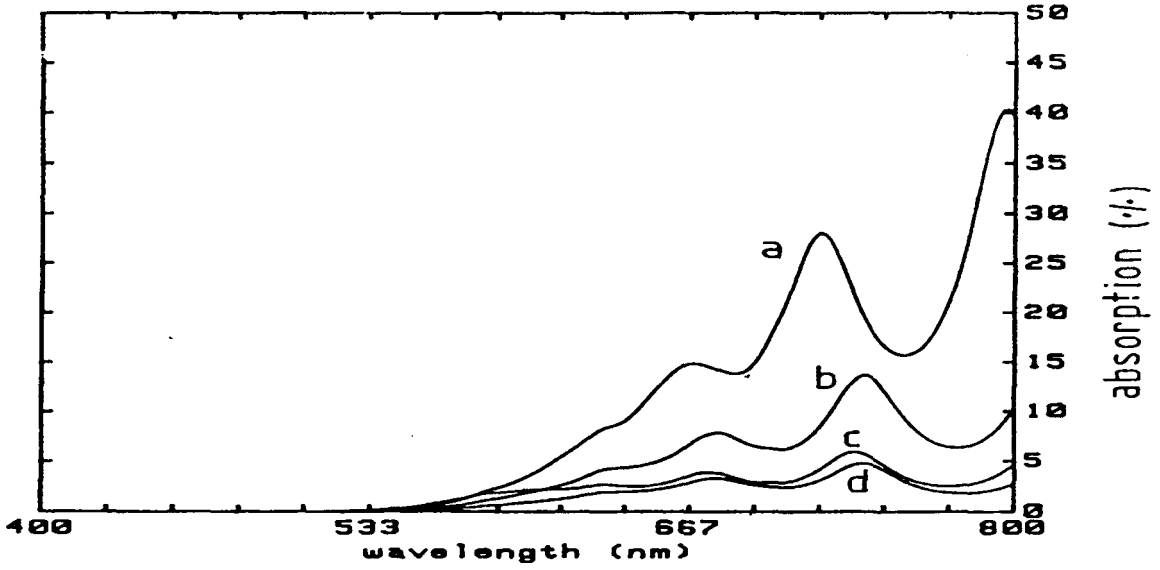

Figure 11. **<u>Computer modeled optical absorption spectra of the bottom electrode in an n-i-p solar cell with quarterwave ITO top contact.</u> The various curves are for a) Al b) Al/ZnO c) Cu/ZnO d)Ag/ZnO. The ZnO is an effective quarterwave thick for 700 nm light. All films are assumed to be smooth.**

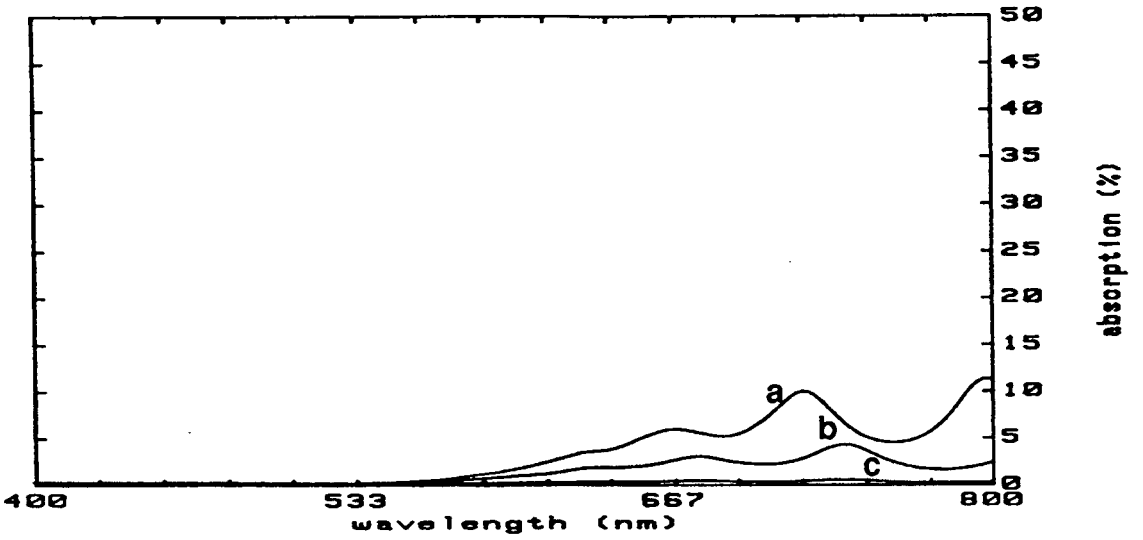

Figure 12. Optical Absorption in a silver electrode. Curve a is absorption in Ag, no ZnO; Curve b is absorption in Ag, coated with 400 Å ZnO; and Curve c is absorption in the ZnO coating. The model assumes a standard p-i-n a-silicon device with microcrystalline silicon n^+ and p^+ layers.

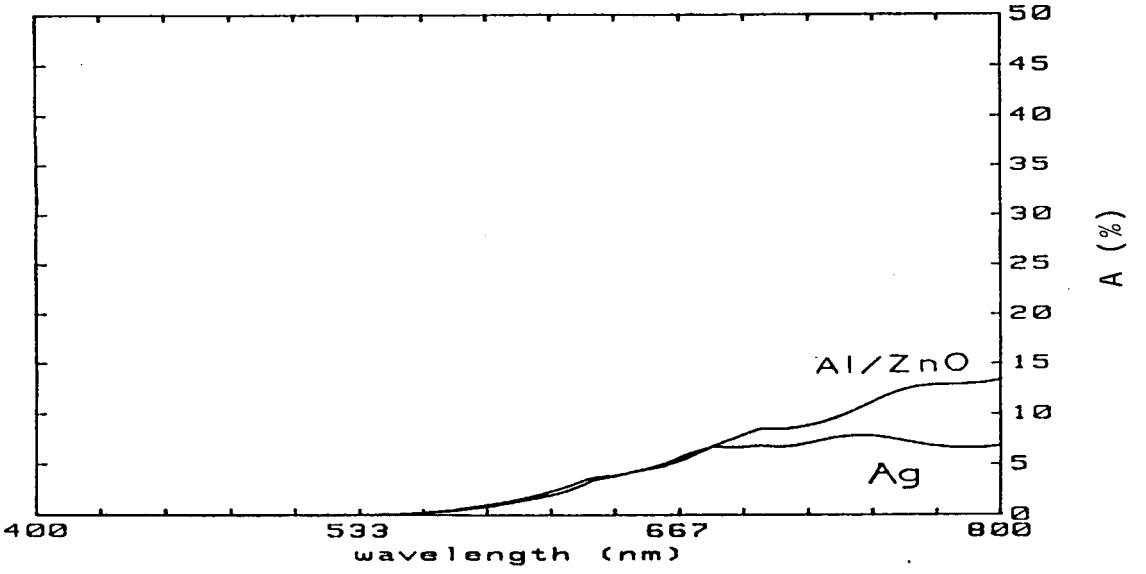

Figure 13. Computer modeled optical absorption spectra of the bottom electrode of an n-i-p solar cell, assuming the incident medium has an index n=4.0. This assumption eliminates most of the optical interference within the device. These two curves show that ZnO enhanced aluminum reflects light almost as well as silver, out to 700 nm. All films are assumed to be smooth.

Figures 11 and 12 are for n-i-p devices coated with a quarterwave thick top contact of indium tin oxide. The interference peaks are from the 5000 angstrom thick silicon i-layer. To eliminate these interference peaks, the device can be modeled as though it were immersed in a non-absorbing medium of index n=4. This was done for the results shown in Figures 13 and 14. Such a system approximates a single pass of light into and back out of the device, i.e. no multiple bounces. On a textured substrate the light would be scattered and experience multiple passes at various angles through the silicon. Thus these results for specular films only serve as a guide for improving the red light response of the devices.

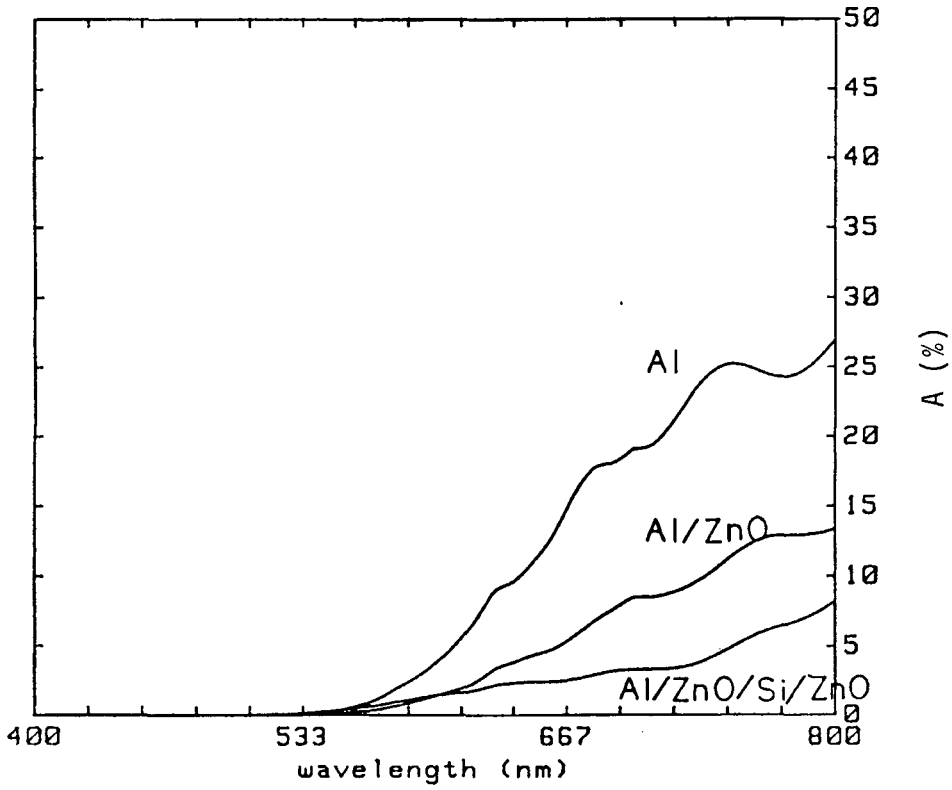

Figure 14. <u>Optical absorption spectra, comparing bare aluminum with single layer dielectric and triple layer dielectric enhanced aluminum films.</u> The triple layer enhanced aluminum absorbs as little light as a single layer enhanced Ag film (see Figure 11, curve d).

The results in Figure 11 show the percentages of light absorbed in bottom electrodes of a) bare aluminum and b), c), and d) aluminum, copper, and silver all enhanced with ZnO. The absorption for bare silver is indicated in Figure 12, top curve. ZnO

enhanced silver is shown again in Figure 12, middle curve, for comparison. The bottom curve in Figure 12, offset slightly from zero, shows the amount of absorption in the ZnO. Also note from Figure 13 that ZnO enhanced aluminum absorbs almost as little light as bare silver, out to 700 nm.

ZnO enhanced silver has the lowest absorption of light of any of the electrode constructions presented here, although a three-layer enhancement film of ZnO/Si/ZnO on aluminum is a close second according to the computer model. For a comparison, see the bottom curves in Figures 11 and 14. The short circuit current densities of solar cells fabricated on textured aluminum and silver substrates, with and without a ZnO enhancement layer, are compared in Table 2. The table lists measured current densities from the devices under both ELH and Xenon light sources adjusted to AM1.5 via a small cell calibrated on the SERI solar simulator.

Table 2. Comparison of Short Circuit Current Densities (mA/cm^2) for devices on various textured metal electrodes.

	Al	ZnO/Al	Ag	ZnO/Ag
ELH Source	13.4	14.5	14.7	16.5
Xenon Source	12.1	13.3	13.4	14.5

Spectral response curves for the same devices are shown in Figure 15, and are compared to a device on specular aluminum. The curve for ZnO enhanced aluminum was very close to that for a silver film, and so is not shown. The response is the same for all samples in the blue and green, but the differences are substantial in the red. From the bottom up, the curves are for devices on 1) specular aluminum, 2) textured aluminum, 3) textured silver, and 4) enhanced textured silver. Textured silver and ZnO/Ag are obtained simply by overcoating a textured aluminum substrate with silver and ZnO. The values in Table 2 and curves in Figure 15 are for a near optimum aluminum texture. A SEM micrograph of this surface is shown in Figure 16, which depicts small spherical metal particles 0.1 to 0.3 micrometer in diameter, scattered on a relatively smooth aluminum base. The total and diffuse reflectance of this surface (coated with Ag), are given in Figure 17, as measured with a Perkin-Elmer Lambda-9 spectrophotometer with an integrating sphere. In the diffuse reflectance measurement, any light scattered outside of a 6 degree x 12 degree window is collected by the integrating sphere. The textured aluminum was grown at 200°C with

250 watts applied to two 4" x 6" aluminum d.c. magnetron targets connected in parallel. The starting base is specular aluminum sputtered from a 5052 aluminum alloy target at room temperature.

Although work is not yet completed on the three-layer dielectric enhanced aluminum substrate (Al/ZnO/Si/ZnO), several results indicate it will work well. ZnO and silicon were sputtered onto specular aluminum and p-i-n devices showed no significant electrical barrier, even without a titanium nitride barrier layer on the aluminum. The silicon layer is phosphine doped and sputtered in an argon/hydrogen atmosphere. Thus a sputtered Al/ZnO/Si substrate has been shown to work electrically and only one additional sputtered layer of ZnO must be added and tested to complete the work on the three-layer dielectric enhancement film.

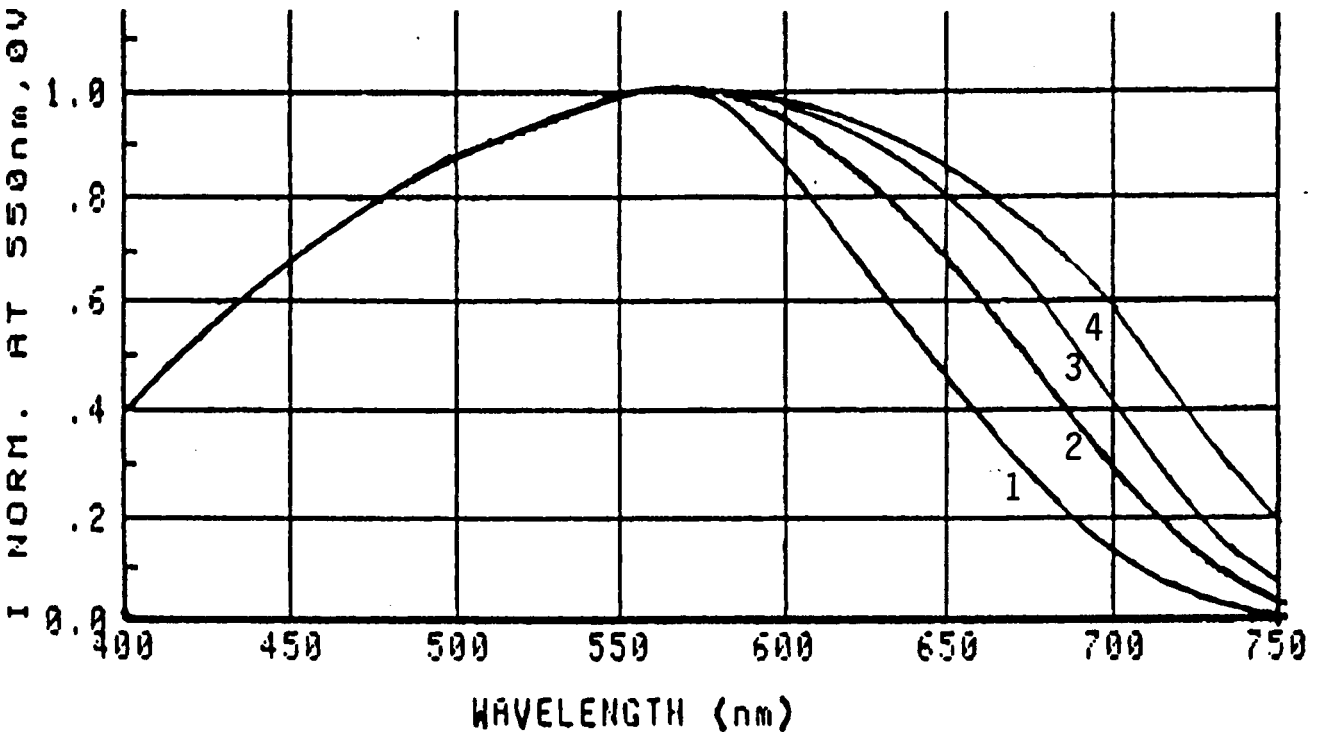

Figure 15. **<u>Spectral response curves for n-i-p a-Si solar cells on specular and various textured surfaces. The response is normalized to 1.0 at the peak efficiency point.</u> The four curves were obtained from samples fabricated on the following electrodes, in order of increasing red light efficiencies: 1) specular aluminum 2) textured aluminum 3) silver coated textured aluminum 4) zinc oxide enhanced textured silver.**

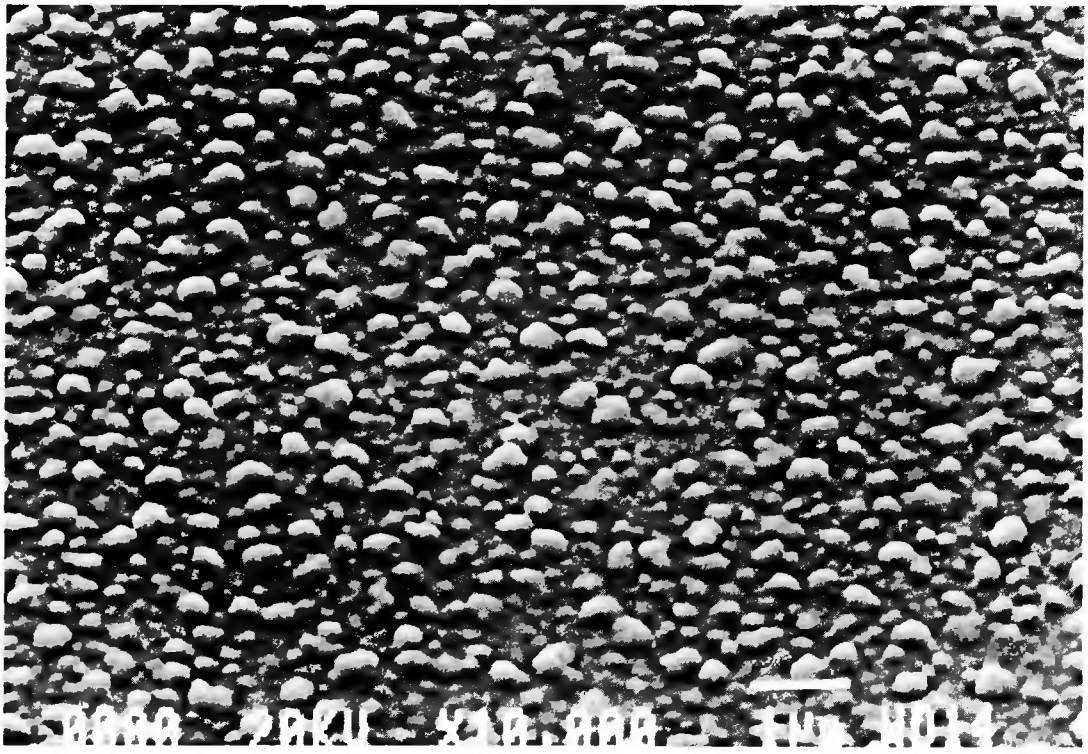

Figure 16. <u>SEM micrograph of the optimum textured aluminum substrate for enhancing the red light response of the n-i-p solar cells.</u> The aluminum was overcoated with approximately 500 angstroms of silver. The aluminum particles are roughly spherical in shape and 1 to 3 thousand angstroms in diameter.

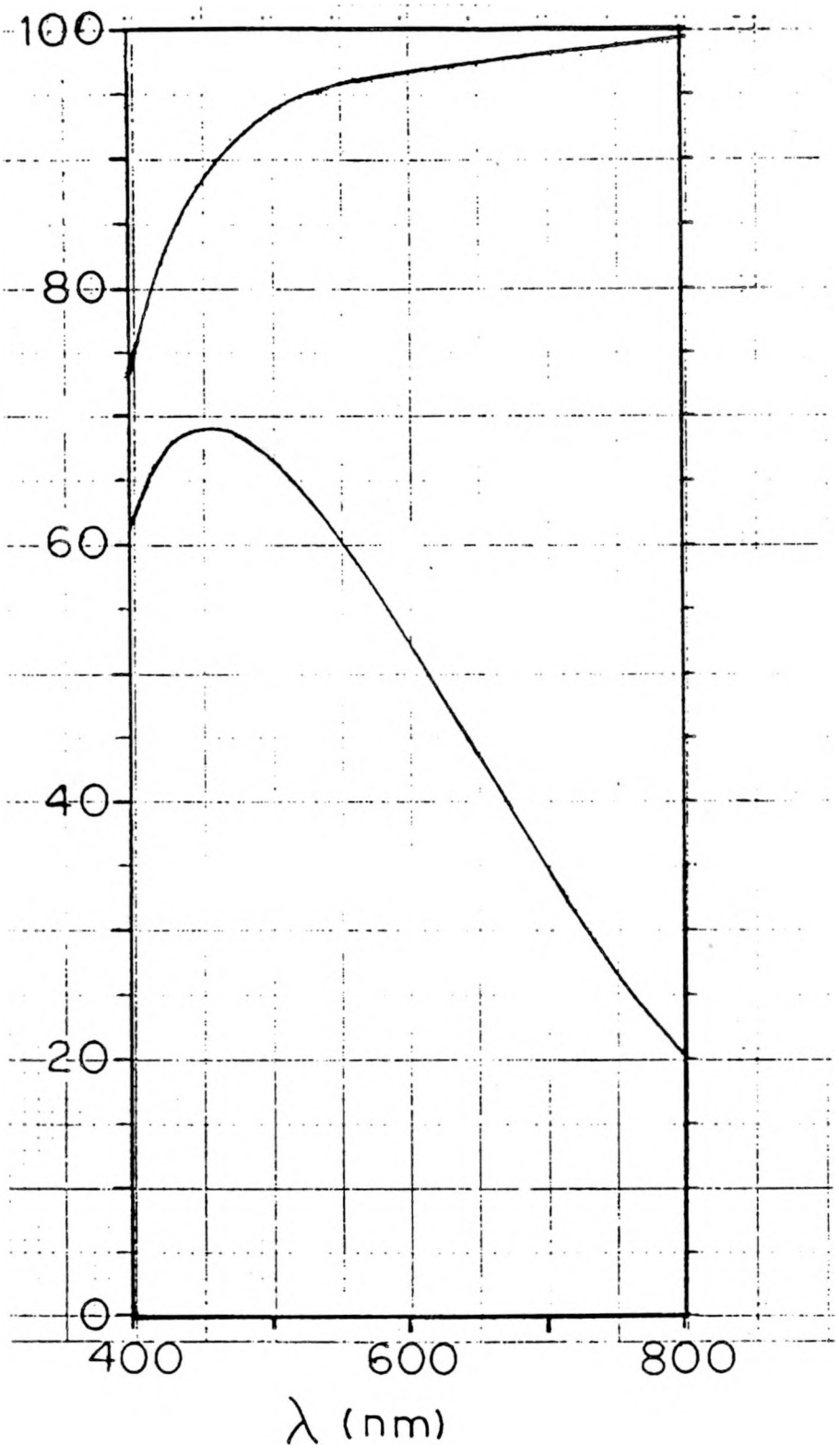

Figure 17. **Total and diffuse reflectance spectra for the silver coated textured aluminum surface shown in Figure 16.**

The success of the optical modeling computer program for previous work indicates that the predicted improvement in reflectance will be realized. For all reflection enhanced substrates, electrical shunts in the devices were found to be a great problem. For this reason, the greatest impediment to improved device efficiency is the high defect density introduced by the addition of these reflection enhancement layers, especially silver. For this reason, the ZnO enhanced Al and the tri-layer ZnO/Si/ZnO enhanced aluminum electrodes are preferred over any electrode containing a silver film. However, both of these structures also have serious shunting problems.

3.4 Reverse Structure Cells and the Multi-Chamber Deposition System

Except for the optical modeling, most of the results and discussion thus far have dealt with p-i-n cells, i.e. cells with the n^+ layer on top, as shown in Figure 1. Research was carried out with this cell structure for several reasons, the main reason being experimental convenience and the speed and reproducibility of small sample deposition in the single-chamber system. This system, and the p-i-n cell structure, allowed us to quickly demonstrate that high quality intrinsic silicon could be fabricated in the presence of a properly treated polyimide web (see Section 3.2). However, the emphasis of this contract is on high efficiency cells produced by a roll-to-roll continuous deposition process. This can only be done with the multi-chamber system, which was described above (see Figure 4). Therefore, once we had demonstrated high quality intrinsic silicon on a polyimide substrate, and after a reliable TCO contact was achieved, all efforts were directed at fabricating high efficiency cells in the multi-chamber system. With such a system, it is equally difficult to fabricate a good p-i-n cell as it is to make a good n-i-p cell. The n-i-p configuration is the obvious choice, however, because it minimizes the effects of light induced degradation.

Two aspects of device fabrication became a problem with the multi-chamber deposition system. The first is fundamental, the second is incidental. The first problem concerns control of the composition of the p/i interface and the second problem has to do with turnaround time or deposition rate. Deposition rate becomes a concern, even for R&D work, because of the distance between the n and p chambers. Upon startup, a total web length of 60 inches has to be coated with silicon films to complete an n-i-p cell only 4 inches long. In the present system, a 5000 Å i-layer deposited at 2.5 Å/second would require a web speed of 0.5 inch/minute, which translates to 2 hours to travel the 60 inches for the first sample. Subsequent samples may take less time depending on which of the five chamber deposition conditions was changed, and the subsequent time lag for the web to traverse the distance between

that particular chamber and the final (p^+) chamber. Therefore, a deposition rate of 5 to 10 Å/minute was virtually mandatory if progress was to be made within the contract time period.

3.4.1 Deposition Rate

The easiest way to increase the deposition rate of silicon from an r.f. discharge of silane gas is to increase the r.f. power to the plasma. However, the electronic quality of the i-layer and, therefore, the fill factor of the device, is inversely proportional to the r.f. power level employed [5, 6]. For production, some trade-off is acceptable; but to produce high efficiency cells, the lowest r.f. power level possible is desirable. One method of achieving a higher deposition rate at lower power levels was reported by Ohnishi et.al. [6], who used magnetic confinement of the plasma. Their method of confinement was adopted, but modified to provide a uniform deposition rate throughout the i-chamber. It was found that excellent uniformity was possible in the 4" x 14" i-layer deposition zone.

The uniformity was achieved by using two magnet arrays, one above the chamber and one below it, as illustrated in Figure 18. This arrangement produces flatter magnetic flux lines through the plasma, with a more uniform field intensity throughout the plasma, than does a single array of magnets above or below the chamber. The magnetic field is approximately 225 gauss throughout the deposition zone between the substrate and r.f electrode. This arrangement also produces several features desirable for manufacturing: no silicon powder formation at up to 10 Angstroms/second deposition rate, and much less sensitivity of deposition rate and powder formation to electrode/substrate separation.

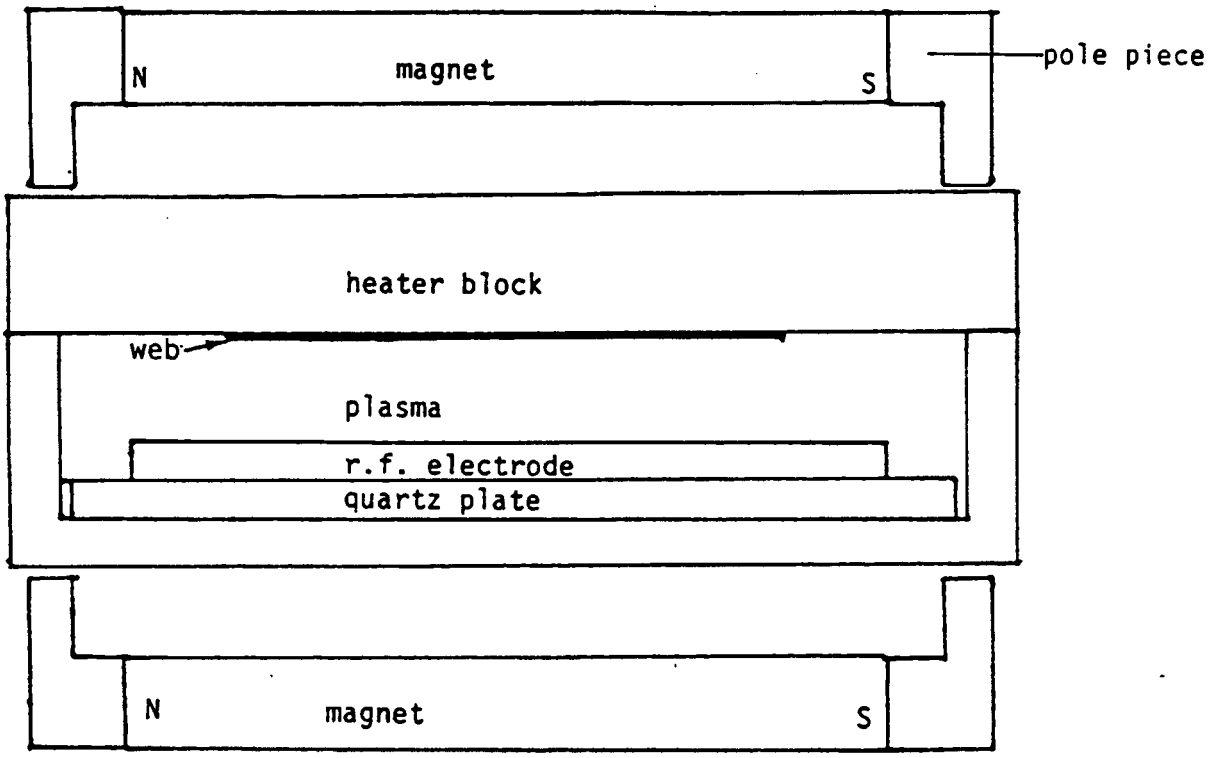

Figure 18. <u>Schematic end view of i-chamber with double magnet array.</u> Web direction is into the page. The bar magnets are arranged perpendicular to the web direction. The pole pieces extend the length of the deposition zone, which is only shown in cross section here.

With the bottom magnet array set for 200 gauss at the r.f. electrode surface, the silicon uniformity was adjusted by varying the number of magnets in the top array. Iron pole pieces assured uniformity along the length of the chamber (not shown). The silicon thickness ratio for the web edge versus center could be adjusted to be less than, greater than, or set equal to 1 by this method.

We observed an even greater enhancement of deposition rate than Ohnishi et. al. reported. For 5Å/second deposition rate, the r.f. power can be lowered from 22.5 watts to 12 watts on a 6" x 14" r.f. electrode if a 200 gauss magnetic field is applied. However, the fill factor did not increase as they reported, with our best cells still showing about a 0.67 fill factor. However, Ohnishi et.al. deposited the p^+ layer first (on glass substrates) in a single-chamber system, while the cells made in this study

are of the reverse structure made in a multi-chamber system. The fill factor of our devices was insensitive to deposition rates up to 7.5 angstroms/second. These results lead us to the conclusion that the fill factor is limited by the composition of the p/i interface, and not by the electronic properties of the i-layer material.

3.4.2 p/i Interface

Purging the i/p^+ transition zone with UHP (99.999% pure) hydrogen had no effect on the open circuit voltage and ff of the devices. This is a little surprising as the i-layer was normally exposed to phosphine and background gases before it entered the p^+ deposition zone. The i/p^+ interface was explored further by replacing the UHP hydrogen with research grade "Matheson" purity hydrogen (99.9999%), doped with 1000 ppm HF gas. A plasma with this gas was used to continually clean the i-layer in the shroud zone as it passed from i and buffer zones to the p^+ deposition zones.

All conditions, with and without a cleaning plasma, with and without a purge gas in the shroud zone, had no effect on the I-V curve of the devices, except for high power etches, which were detrimental to the devices. These results lead us to the conclusion that a high open circuit voltage and ff of our n-i-p cell will require some type of dopant profiling near the p/i interface. Ultra-pure deposition conditions alone are not sufficient conditions. Currently, with a microcrystalline p^+ layer without carbon, and with no profiling, the $V_{o.c.}$ is 0.89 volt and the best fill factors are 0.67 to 0.68. In the single-chamber system, with no profiling of an n-i-p device, a $V_{o.c.}$ of 0.94 volt was reproducibly achieved, but with a fill factor of only 0.50.

4.0 CONCLUSIONS

We have demonstrated that a-Si devices with fill factors over 0.70 can be deposited on metallized polyimide substrates. No long term static bakeout of the polyimide was required.

Problems with contact resistance of the SnO_2/ITO contact were eliminated by switching to ZnO as the transparent conducting top contact. In addition, the ZnO conductivity was improved to produce a TCO of 8 to 9 ohms/square sheet resistance with less than 8 percent average optical absorption from 400 to 800 nm. Following these improvements, p-i-n cells with fill factors above 0.70 were routinely fabricated in the single-chamber system. (The highest efficiency measured on a p-i-n device was 8.36%.)

Progress was also made in improving the red light response of the cells. Dielectric enhanced metal reflecting electrodes increased the short circuit current density by over 1mA/cm^2. In addition, a three-layer dielectric mirror coating was designed which can increase the current density by an additional 1mA/cm^2, but this has not yet been demonstrated in a device. Thin-film defects, which cause electrical shunts, were found to be a major obstacle to implementing enhanced reflection electrodes in our devices.

Although high fill factors were achieved with p-i-n devices made in a single-chamber system, stability and manufacturing requirements demand an n-i-p cell which is fabricated on a continuously moving substrate in a multi-chamber system. The latter devices are currently limited by fill factors of 0.67 and open circuit voltage of 0.89 volt. The overall goal of 10% efficiency for a small-area device made by this technique was not achieved.

One significant breakthrough made under this contract was the development of a magnetic confinement scheme for the i-layer plasma which can produce uniform and high deposition rates up to 10Å/second over large areas with no powder generation within the i-chamber. This technique permits the use of lower r.f. power levels which can improve the fill factor, provided the problems of the p/i interface can be solved in a continuous web deposition system.

5.0 REFERENCES

1. C.K. Lau, S.K. Tiku, and K.M. Lakin, J. Electrochem.Soc 127, (1980) 1843
2. J.F. Dewald, Bell System. Techn. J., 39, (1960) 615
3. J.F. Dewald, J. Phys. Chem. Solids, 14, (1960) 155
4. J.F. Dewald, J. Phys. Chem. Solids, 17, (1961) 344
5. H. Chatham and P.K. Bhat, Glasstech Solar, Inc., SERI Final Technical Report, April 1989, Subcontract No. ZB-7-06002-1
6. M. Ohnishi et.al., Jap. J. Appl. Phys., 27, (1988) 40

Document Control Page	1. SERI Report No. SERI/TP-211-3656	2. NTIS Accession No. DE90000314	3. Recipient's Accession No.

4. Title and Subtitle
Improvement of Small Area Amorphous Silicon Thin Film Photovoltaics on Polymer Substrate, Final Subcontract Report

5. Publication Date
February 1990

6.

7. Author(s)
M.F. Weber

8. Performing Organization Rept. No.

9. Performing Organization Name and Address
Information and Imaging Technologies
Sector Laboratories / 3M
St. Paul, Minnesota 55144-1000

10. Project/Task/Work Unit No.

11. Contract (C) or Grant (G) No.
(C) ZB-8-07271-1
(G)

12. Sponsoring Organization Name and Address
Solar Energy Research Institute
1617 Cole Boulevard
Golden, Colorado 80401-3393

13. Type of Report & Period Covered
Technical Report

14. 1 March 88 - 30 June 89

15. Supplementary Notes
SERI Technical Monitor: W. Luft, (303) 231-1823

16. Abstract (Limit: 200 words)

This report describes a contract to produce, using roll-to-roll deposition on polyamide substrate, a small-area amorphous-silicon p-i-n photovoltaic (PV) cell with an energy conversion efficiency of 10% under air mass 1.5 insolation. Three improvements were attempted to achieve this goal: (1) zinc oxide, a transparent conducting oxide, was used as a top contact; the zinc oxide conductivity was improved to 8-9 ohms/square sheet resistance with less than 8% average optical absorption. (2) The red light response was improved with dielectric enhanced metal reflecting electrodes, which increased the short-circuit current density by more than 1 mA/cm^2; a three-layer dielectric mirror coating was also designed that can increase the current density by another 1 mA/cm^2. (3) Improving the fill factor of the n-i-p (reverse structured) devices was also achieved in a multichamber deposition system. The overall energy conversion efficiency of the PV cell was 8.36%. Major obstacles to higher efficiencies are (1) controlling the thin-film defects that cause electrical shunts in devices fabricated on enhanced reflection electrodes, and (2) controlling impurities and introducing dopant profiles near the p/i interface in a continuous web deposition system.

17. Document Analysis

a. Descriptors Photovoltaics ; thin films ; amorphous silicon ; efficiency

b. Identifiers/Open-Ended Terms

c. UC Categories 271

18. Availability Statement
National Technical Information Service
U.S. Department of Commerce
5285 Port Royal Road
Springfield, VA 22161

19. No. of Pages
38

20. Price
A03

Form No. 0069 (3-25-82)